Supporting Information

Nanostructured Few−Layer Graphene with Superior Optical Limiting Properties Fabricated by a Catalytic Steam Etching Process

Zhenyu Sun,[a] Ningning Dong,[b] Kunpeng Xie,[a] Wei Xia,[a] Dennis König,[c] Tharamani Chikka Nagaiah,[d] Miguel D. Sánchez,[a,e] Petra Ebbinghaus,[f] Andreas Erbe,[f] Xiaoyan Zhang,[b] Alfred Ludwig,[c] Wolfgang Schuhmann,[d] Jun Wang,[b] and Martin Muhler*[a]*

[a] Laboratory of Industrial Chemistry, Ruhr-University Bochum, D-44780, Bochum, Germany

[b] Department Key Laboratory of Materials for High-Power Laser, Shanghai Institute of Optics and Fine Mechanics, Chinese Academy of Sciences, Shanghai 201800, China

[c] Department of Mechanical Engineering, Institute for Materials, Ruhr-University Bochum, D-44780, Bochum, Germany

[d] Analytische Chemie-Elektroanalytik & Sensorik, Ruhr-University Bochum, D-44780, Bochum, Germany

[e] Departamento de Física and Instituto de Física del Sur, Universidad Nacional del Sur-CONICET, 8000, Bahía Blanca, Argentina.

[f] Max-Planck-Institut für Eisenforschung GmbH, Max-Planck-Str. 1, 40237, Düsseldorf, Germany

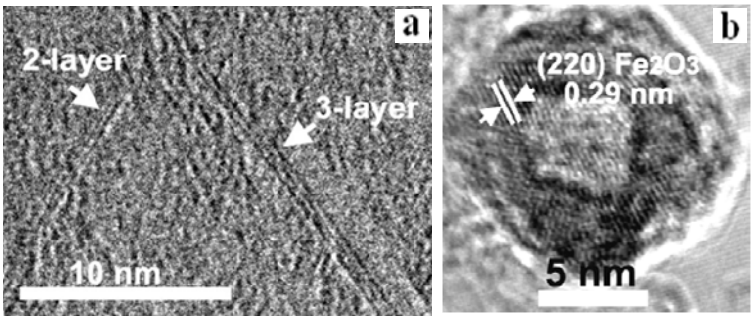

Figure S1. (a) TEM image of pristine graphene. (b) HRTEM image of an individual iron nanoparticle deposited on graphene after etching. The lattice spacing of about 0.29 nm corresponds to the (220) plane of a cubic iron oxide spinel structure. This contrasts with the (110) plane of α−Fe_2O_3 with a lattice spacing of 0.25 nm for the NPs before etching (inset in Figure 1b).

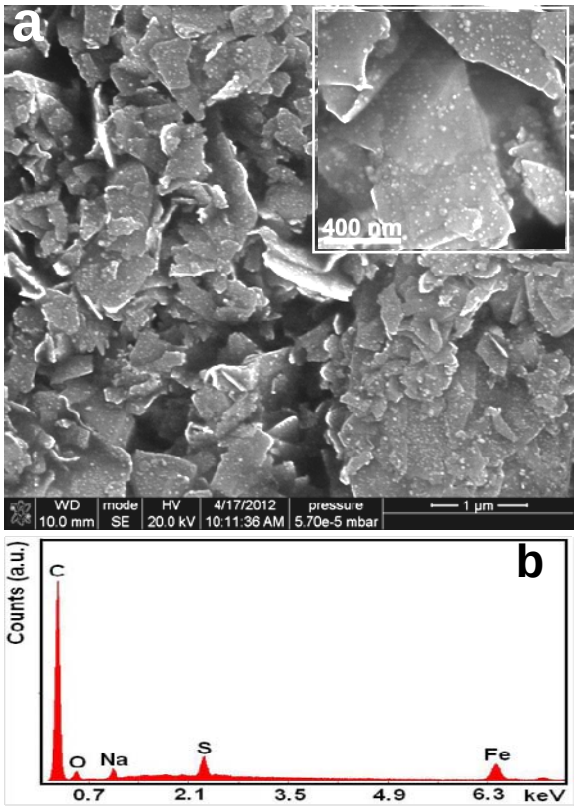

Figure S2. (a) SEM image of graphene sheets decorated with iron oxide NPs after steaming at 650 °C for 30 min. Inset: An enlarged view of the sample. (b) EDX pattern of the sample shown in a, which indicates the presence of iron and oxide arising from the NPs. The elements of Na and S originate from the sample holder used for SEM measurements.

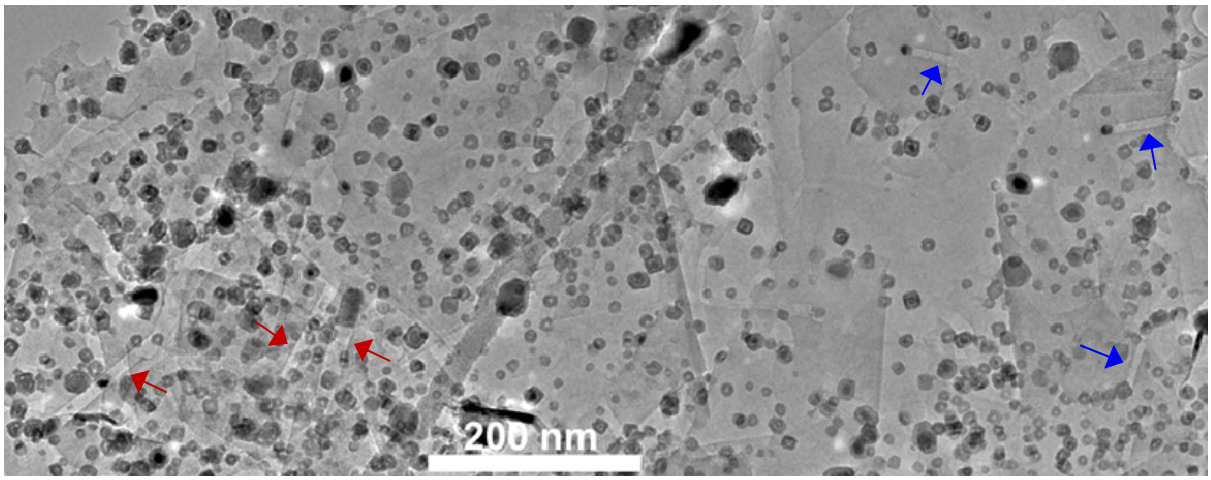

Figure S3. TEM image of graphene sheets after catalytic steaming at 650 °C for 30 min. Larger catalyst NPs appear to channel longer trenches (illustrated by arrows in red) compared to smaller NPs (illustrated by arrows in blue).

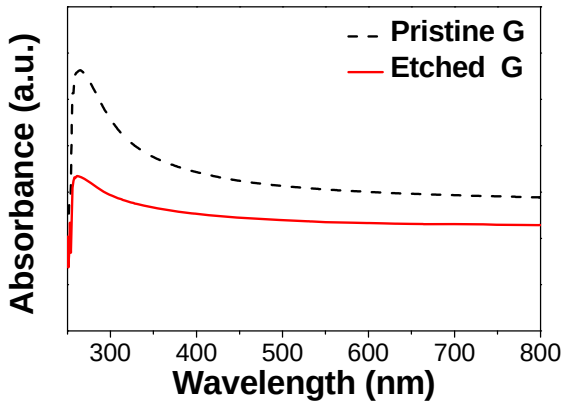

Figure S4. UV−vis absorption spectra of suspended graphene in *i*−PrOH before and after etching (650 °C, 0.3 mL min^{-1} H_2O vapor).

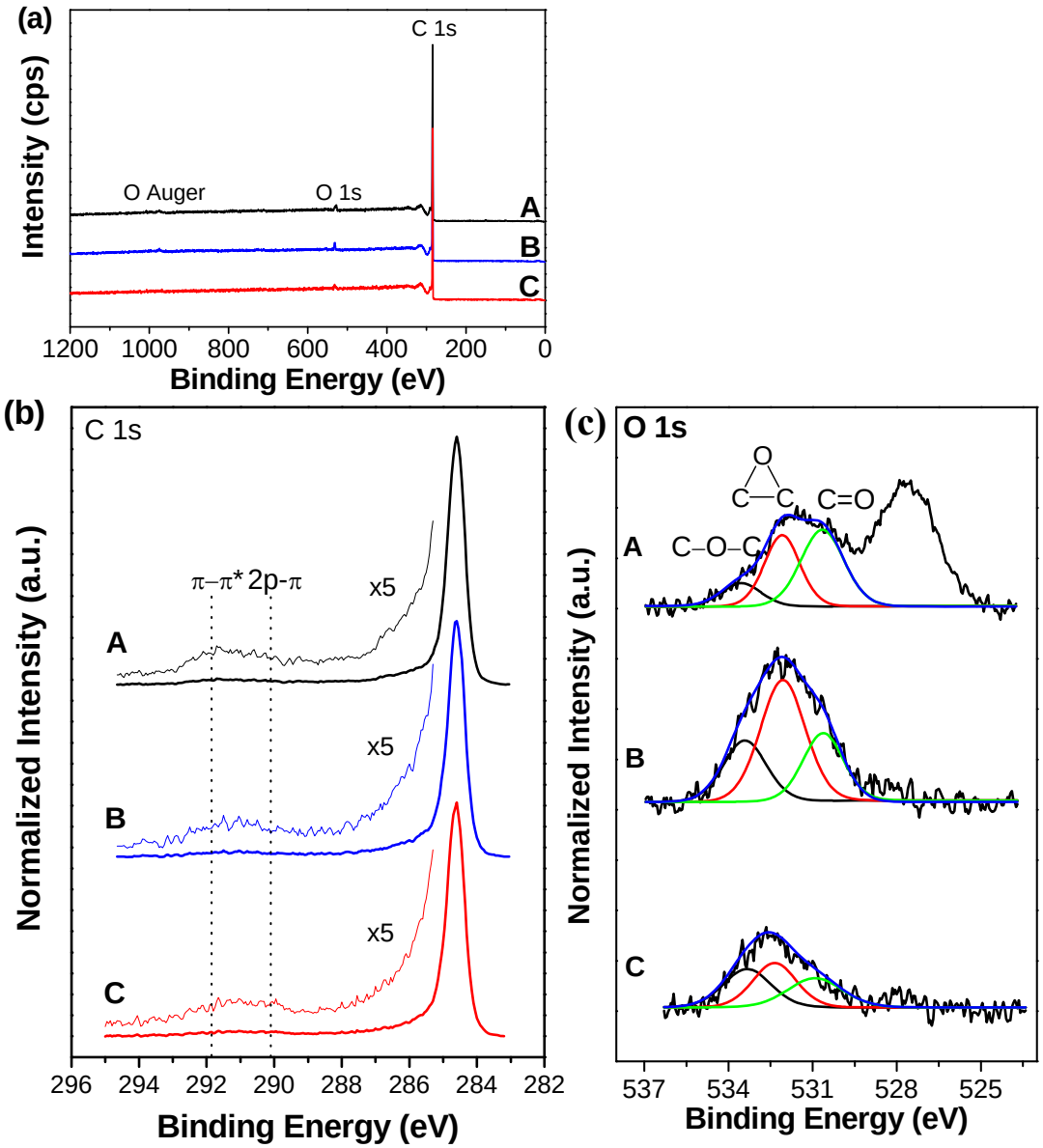

Figure S5. (a) Wide survey, (b) C 1s, and (c) O 1s XPS spectra of graphite (A) and graphene before (B) and after (C) steaming (650 °C, 0.3 mL min^{-1} H_2O vapor).

For quantification of surface oxygen in original graphite and graphene, XPS spectra for the O 1s region were taken (Figure S5c). There are a number of different oxygen functional groups, as described elsewhere,[1-2] which are mainly divided into three groups according to the C–O bonding type as: C=O (ketones, aldehydes, quinones), C–O–C (phenols and ethers), and epoxides.[1-3] Oxygen atoms in esters, carboxyls, anhydrides, and pyrones have both single bonds and double bonds with carbon atoms contributing to both peaks.[2] Aside from the three peaks centered at 530.7, 532.1 and 533.5 eV corresponding to C=O, epoxy, and C–O–C groups,[4] a prominent peak can be also observed at the low binding energy side of the graphite sample (trace A in Figure S5c). This signal cannot be assigned to any oxygen functional group and was assumed as a contaminant arising from the commercial manufacturing process. On the basis of the deconvoluted O 1s XPS spectra, the atomic percentage of oxygen was calculated from the corresponding peak areas.

The relative intensities and widths of D (~1350 cm^{-1}) and G (~1580 cm^{-1}) bands in the Raman spectra have been used to obtain a wealth of structural information on graphene and graphitic materials. When analysing "intensities" in spectroscopy, there are always two possibilities: using the maximum value *M* at the ordinate axis, or using integrated intensities *A*. When analysing ratios, the two possibilities yield the same result if the broadening mechanism of the peaks is independent of the ratio. As in the case of the Raman D and G bands, the width is strongly affected by Raman-active defects, and differences are expected when comparing data based on *M* and *A*. Complicating the analysis, for the determination of areas, several options exist: an integration of the spectrum above a baseline or a peak fit with one of several possible shapes, the most popular being Lorentzian and Gaussian. The treatment of the baseline might also affect the resulting ratios. We will discuss the differences

that result from different analysis procedures for the spectra of samples from this work. All spectra were measured using excitation at 633 nm (1.96 eV).

Based on the work of Tuinstra and Koenig,[5] the intensity ratio between D and G band is related to the crystallite size L_a as determined by X−ray diffraction. Based on band area ratios, Cançado et al.[6] established a quantitative empirical relation, including the dependence on excitation energy. The resulting relation yields L_a in nm with an excitation energy E_i in eV as $L_a = 560(A_D/A_G)^{-1}/E_i^4$

For the sample of pristine graphene, analysed at several points, A_D/A_G is ~ (1.07±0.05) fitting each peak individually with a Gaussian peak shape, or A_D/A_G is ~1.6 fitting the spectrum with Lorentzian peaks. The resulting values for L_a are (36±2) nm and ~24 nm, respectively. Gaussian peak shape rather than Lorentzian results in better fits of the spectra, which can be attributed to the distribution of peak maxima from slightly different local environments over the illuminated spot. The treatment of baseline and residual intensity between and at the fringes of the peaks causes variability of the resulting ratios on the same level as the differences between Gaussian and Lorentian peak shape, *i.e.* a factor of 1.5. When using peak heights instead of areas, M_D/M_G is ~ (0.58±0.08), resulting in a significantly higher L_a of (66±9) nm when plugged into the equation from Cançado et al.

The same trends are found for the sample of etched graphene. While before steaming, the Lorentzian peak shape yielded rather poor fits, after treatment the spectra can be easily fit using a Lorentzian peak shape, and only small differences between the usage of Lorentzian or Gaussian shape are observed. Using Gaussian peak shape, A_D/A_G is ~ (1.6±0.2) resulting in L_a ~ (24±3) nm, while with Lorentzian peak shapes A_D/A_G is ~ (1.7±0.2) resulting in L_a ~ (23±3)

nm. When analysing peak heights instead of peak areas, M_D/M_G is ~ (0.95±0.08), yielding L_a ~ (40±3) nm.

Ignoring the data using Lorentzian peak fits of the pristine graphene due to the bad fits, the numbers differ substantially between the use of area ratios and peak maximum ratios. The trend within this series of samples is, however, independent of the method. Furthermore, the resulting L_a is a factor of ~1.75 (within the error given in ref. 6) too high when using M rather than A in equation 1 from ref. 6. Postulating the same energy dependence as in ref. 6 and extending their approach, we therefore suggest to use the following equation for determination of L_a from peak height: $L_a = 560(A_D/A_G)^{-1}/E_i^4 = 320(M_D/M_G)^{-1}/E_i^4$. For quantifying the distance L_D between Raman–active defects, ref. 7 discusses explicitly the use of peak maxima instead of peak areas. Therefore, no discussion is presented here on the role of defects on L_D.

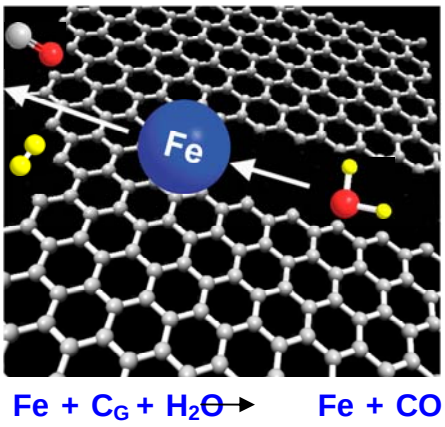

Figure S6. Schematic illustration of the etching process of few−layer graphene. The sizes of the NP, molecules of H_2O, CO, and H_2 in the figure are only illustrative and are not scaled with the graphene molecular structure.

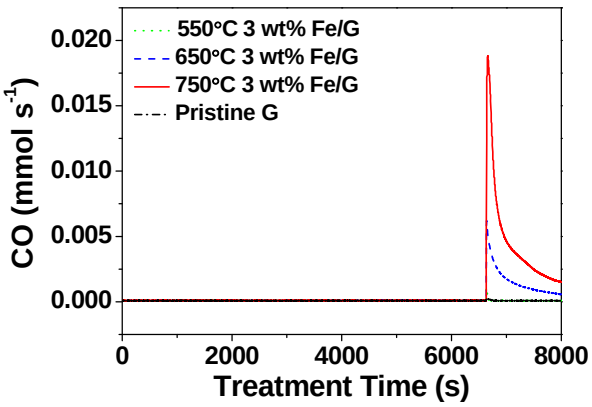

Figure S7. The production rate of CO as a function of reaction time during the gasification at different temperatures.

1 Schlögl, R. Carbons. In *Handbook of Heterogeneous Catalysis*, G. Ertl, H. Knözinger, F. Schüth, J. Weitkamp, Eds. Wiley VCH Verlag: Weinheim, **2008**; Vol. *1*, 357−427.

2 Kundu, S.; Wang, Y. M.; Xia, W.; Muhler, M. Thermal Stability and Reducibility of Oxygen-Containing Functional Groups on Multiwalled Carbon Nanotube Surfaces: A Quantitative High-Resolution XPS and TPD/TPR Study. *J. Phys. Chem. C* **2008**, *112,* 16869−16878.

3 Larciprete, R.; Lacovig, P.; Gardonio, S.; Baraldi, A.; Lizzit, S. Atomic Oxygen on Graphite: Chemical Characterization and Thermal Reduction. *J. Phys. Chem. C* **2012**, *116,* 9900−9908.

4 Fairley, N. Casa XPS Version 2.3.15, copyright 1999-2009 Casa Software Ltd.

5 Tuinstra, F.; Koenig, J. L. Raman Spectrum of Graphite. *J. Chem. Phys.* **1970**, *53,* 1126−1130.

6 Cançado, L. G.; Takai, K.; Enoki, T.; Endo, M.; Kim,Y. A.; Mizusaki, H.; Jorio, A.; Coelho, L. N.; Magalhães-Paniago, R.; Pimenta, M. A. General Equation for the Determination of the Crystallite Size L-a of Nanographite by Raman Spectroscopy. *Appl. Phys. Lett.* **2006**, *88*, 163106.

7 Cançado, L. G.; Jorio, A.; Martins Ferreira, E. H.; Stavale, F.; Achete, C. A.; Capaz, R. B.; Moutinho, M. V. O.; Lombardo, Kulmala, A. T. S.; Ferrari, A. C. Quantifying Defects in Graphene via Raman Spectroscopy at Different Excitation Energies. *Nano Lett.* **2011**, *11*, 3190−3196.